Molecular-level insight into the impact of different dissolved organic matter on the aggregation, dissolution and sedimentation of Zn-doped CdTe quantum dots

Jing Wang[a], Jiaxuan Li[a], Xinyi Peng[b], Wenbin Mu[b], Shuyang Guo[a], Songrui Yang[a], Xinping Yu[a], Lining Zhao[b]

[a]School of Environmental and Material Engineering, Yantai University, 30# Qingquan Road, Yantai 264005, P. R. China

[b]College of Life Science, Institute of Life Science and Green Development, Hebei University, Baoding, 071002, P.R. China

*All correspondence should be addressed to:

Lining Zhao

College of Life Science, Institute of Life Science and Green Development,

Hebei University, Baoding, Hebei, 071002, China.

Email: liningzhao@hbu.edu.cn

Paper Summary

Characters with spaces: 4990

Number of figures: 6

Number of tables: 0

1. The method of calculating the particle size and concentration of QDs

The particle size and concentration of QDs were calculated according to the study of Yu et al. (2003). The first maximum value of the UV-vis absorbance spectrum was used to determine the particle size of QDs, and the formula was as follows：

$$D = (9.8127*10^{-7})\ \lambda^3 - (1.7147*10^{-3})\ \lambda^2 + (1.0064)\ \lambda - 194.84 \quad (1)$$

$$A = \varepsilon CL \quad (2)$$

$$\varepsilon = 10043(D)^{2.12} \quad (3)$$

where λ is the wavelength of the first absorbance peak in the UV-vis absorbance spectra, D is the size of QDs, A is the absorbance value of the first peak in the UV-vis spectrum of QDs, ε is the molar absorptivity at the first absorbance peak, C is the molar concentration of QDs, and L is the length of the cuvette.

2. The synthesis methods of N-acetyl-L-cysteine (NAC)-capped CdTe: Zn^{2+}QDs

Firstly, $CdCl_2$ (0.1 M, 6 mL), N-acetyl-L-cysteine (NAC, 0.17 g) and deionized water (90 mL) were added into a three-necked flask (100 mL), which was kept in an oil bath at 100℃. Different volumes of $ZnCl_2$ (0.1 M) were added into the flask according to the Zn/Cd doping ratios of 1%, 5% and 10%. After stirring at room temperature for 5 min, NaOH (1.0 M) was added into the flask to adjust the value of pH to 10.0. Then $NaBH_4$ (0.15 g) and Na_2TeO_3 (0.02 M, 6 mL) were quickly added into the flask and reacted for 10 min. The reaction solution was taken out after refluxing for 2 h. The solution was added with ethanol with a volume ratio of 2:1 and then centrifuged (8000 rpm, 5 min) for the purification. NAC-CdTe: Zn^{2+} QDs powder was obtained after drying the precipitate in vacuum overnight.

3. The characterization methods of NAC-capped CdTe: Zn^{2+} QDs

After purification and drying overnight, CdTe: Zn^{2+} QDs powder was obtained and then dispersed in deionized water for measuring fluorescence spectra on a F-4600 fluorophotometer (Hitachi, Japan) and UV-vis absorbance spectra on a UV-2450 spectrophotometer (Shimadzu, Japan). Transmission electron microscope (TEM, JEM-1400plus, JEOL, Japan), X-ray diffraction (XRD, XRD-7000X, Shimadzu, Japan) and

FTIR (IR Prestige-21, Shimadzu, Japan) were utilized to characterize the crystal phase structure, morphology and chemical bond, respectively. The atomic valence and elemental composition of the samples were studied by X-ray photoelectron spectroscopy (XPS, ESCA LAB250Xi, Thermo Fisher Technology, US), and energy dispersive X-ray spectrometer (EDS) of a scanning electron microscope.

4. The characterization results of NAC-capped CdTe: Zn^{2+} QDs

The fluorescence emission spectra and the UV-visible absorbance spectra of N-acetyl-L-cysteine (NAC) capped CdTe: Zn^{2+} QDs are presented in Fig. S1 and Fig. S2. QDs fluorescence has a narrow and symmetric peak in Fig. S1, indicating that the particle size of the synthetic CdTe: Zn^{2+} QDs is relatively uniform. The calculated particle size of QDs is 3.02 nm according to the above method and Fig.S2. The XRD pattern of CdTe: Zn^{2+} QDs are shown in Fig. S3. As shown in Fig.S3, CdTe: Zn^{2+} QDs has high purity and good crystallization properties. It has three distinct diffraction peaks, which corresponds to the three crystal planes (111), (220), and (311) planes of CdTe lattice (Yu et al., 2012). The TEM images of CdTe: Zn^{2+} QDs are presented in Fig. S4 and exhibit a good dispersion. Both well-resolved lattice plane and the interplanar distance of 0.35 nm could correspond to the (111) plane in Fig. S3, further confirming the successful synthesis of CdTe: Zn^{2+} QDs. The FTIR spectra of NAC and CdTe: Zn^{2+} QDs are shown in Fig.S5. The characteristic absorbance peaks around 3462 cm^{-1} and 2372 cm^{-1} were major infrared absorption band of -OH stretching vibration and C-N stretching vibration, respectively. Compared with the spectrum of NAC molecule, the characteristic absorbance peaks of $-COO^-$ around 1411 cm^{-1} (sv COO^-) and 1717 cm^{-1} (mv COO^-), as well as –SH around 2547 cm^{-1} disappeared in the spectrum of CdTe: Zn^{2+} QDs; while the absorbance band of -COOM (1635 cm^{-1} and 1386 cm^{-1}) appeared. These results indicated that Cd^{2+} of CdTe: Zn^{2+} QDs surface formed covalent bonds with carboxyls and thiols, implying that CdTe: Zn^{2+} QDs were successfully coated by NAC molecules. In Fig. S6, the characteristic peaks of Cd3d, Te3d and Zn2p were observed in the XPS results of CdTe: Zn^{2+} QDs. The existence of Zn^{2+} in CdTe: Zn^{2+} QDs could be confirmed by the appearance of characteristic Zn2p

peaks at 1021.52 and 1044.56 eV. The constituent elements of CdTe: Zn^{2+} QDs surface are shown in EDS results (Fig. S7), further proving the existence of Cd, Te and Zn elements in CdTe: Zn^{2+} QDs.

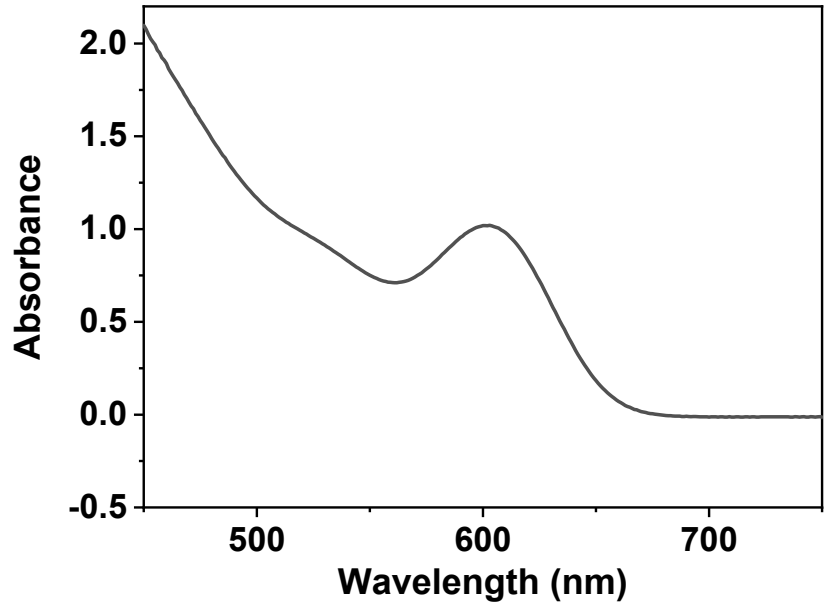

Fig. S1 UV-vis spectra of CdTe: Zn^{2+} QDs.

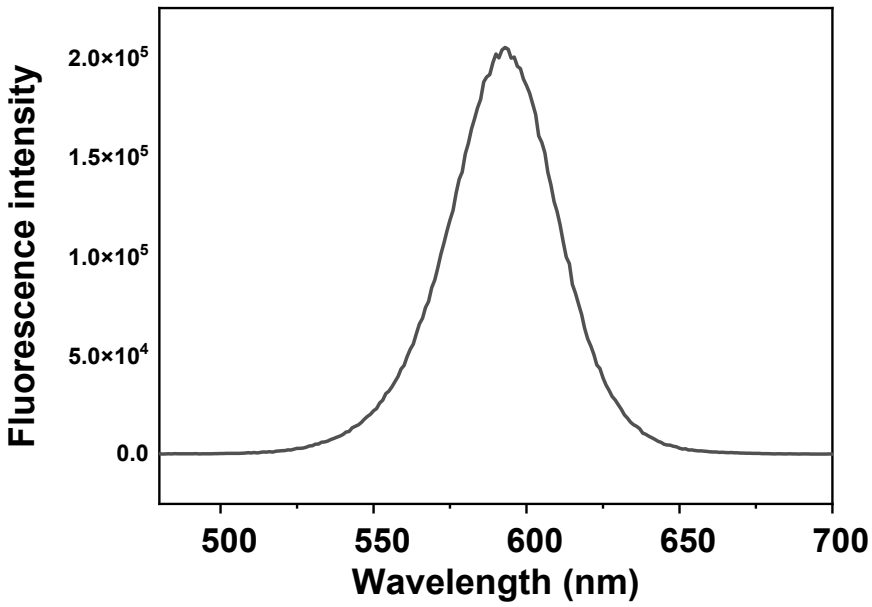

Fig. S2 Fluorescence spectra of CdTe: Zn^{2+}QDs.

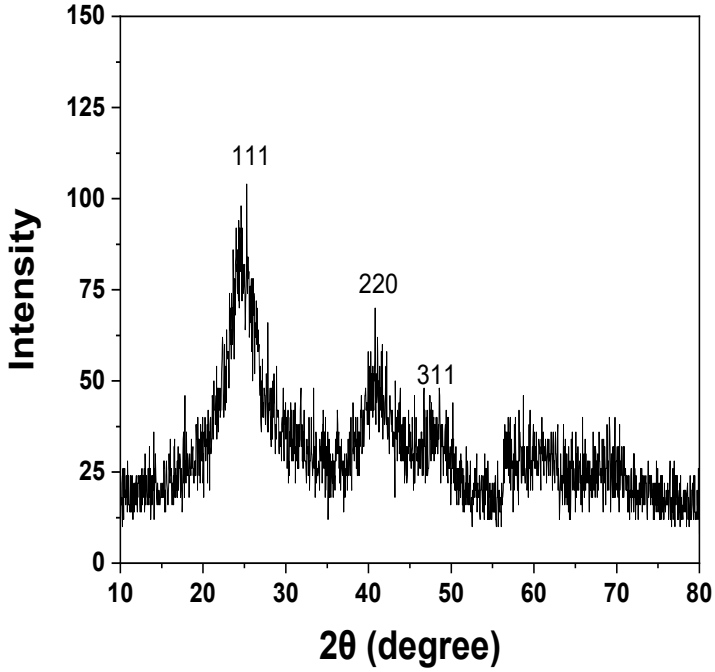

Fig. S3 XRD patterns of CdTe: Zn^{2+}QDs

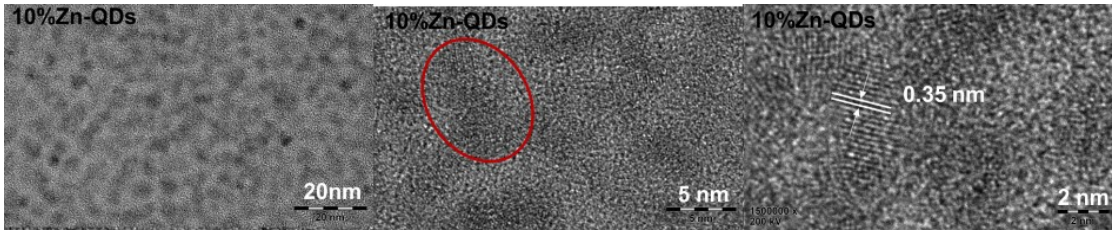

Fig. S4 TEM image of CdTe: Zn^{2+}QDs

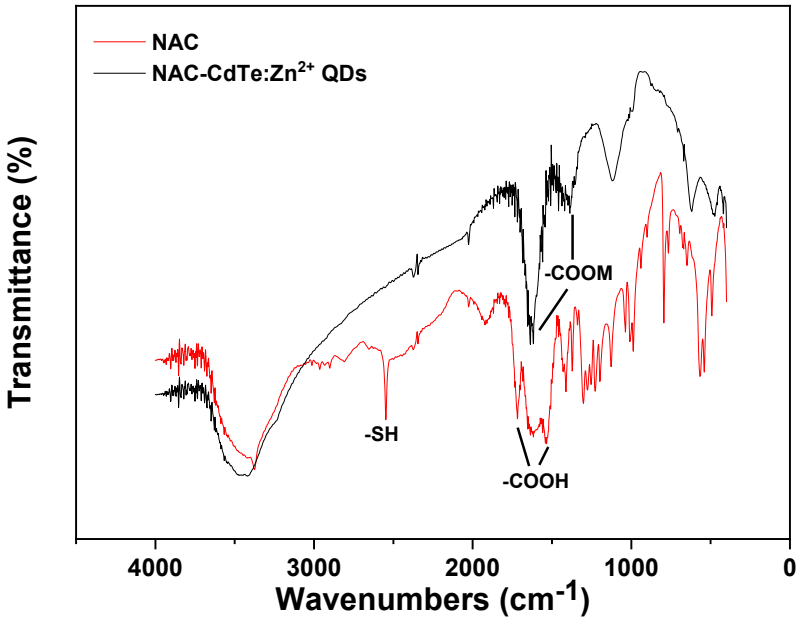

Fig. S5 FTIR spectra of NAC and NAC-CdTe: Zn^{2+}QDs

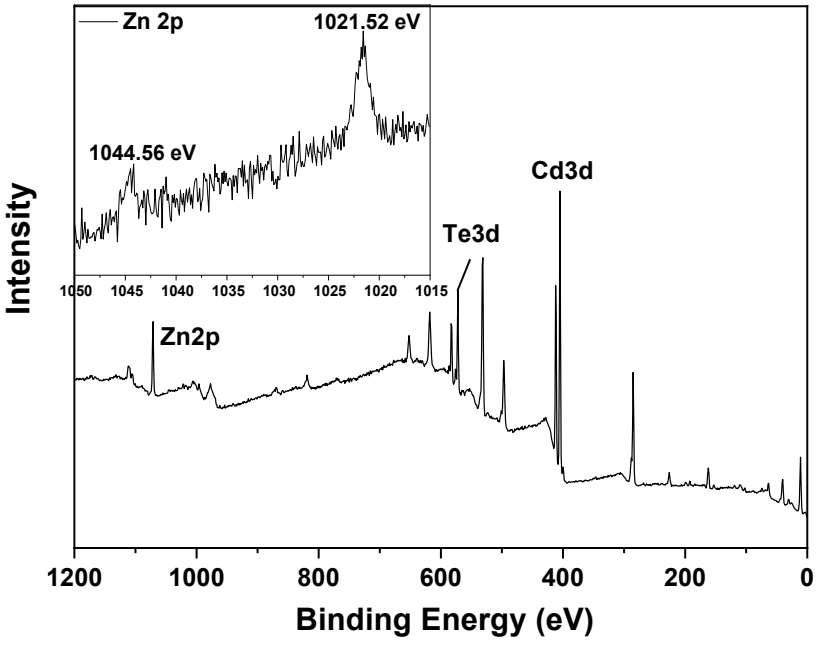

Fig.S6 The XPS results of CdTe: Zn^{2+}QDs

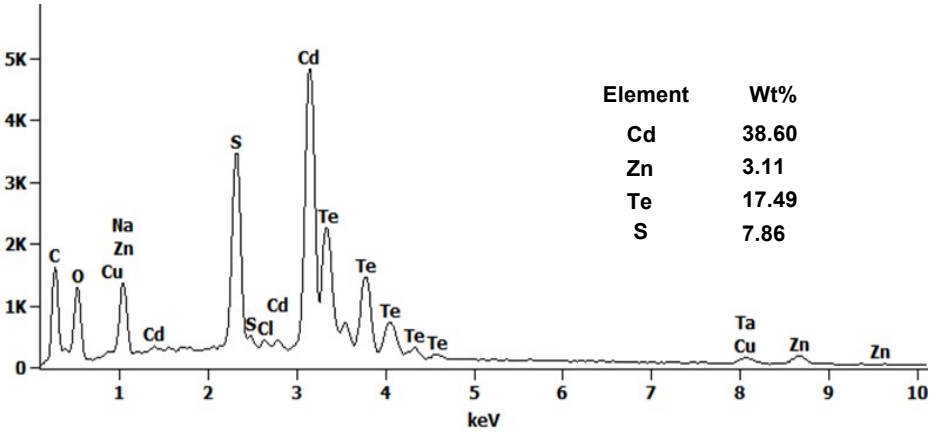

Fig.S7 The EDS results of CdTe: Zn^{2+}QDs

Table S1 The components of artificial water.

Components	Freshwater	Seawater
NaCl (g/L)	-	16.3
Na_2SO_4 (g/L)	-	2.6
KCl (mg/L)	3	457.5
$NaHCO_3$ (mg/L)	72	127.5
KBr (mg/L)	-	66
$Na_2B_4O_7$ (mg/L)	-	13.5
$MgCl_2$ (g/L)	-	3.3
$CaSO_4$ (mg/L)	35.6	-
$MgSO_4$ (mg/L)	45	-
$CaCl_2$ (g/L)	-	0.7
$SrCl_2$ (mg/L)	-	8.9

Table S2 Thermodynamic characteristics and binding affinities for QDs-DOM interactions

DOM	N	K (M^{-1})	ΔH (J mol^{-1})	ΔS (J mol^{-1} K^{-1})	ΔG (kJ mol^{-1})
HA	6.29	3.05×10^{5}	3.44×10^{4}	220.5	-31.3
FA	4.55	1.85×10^{6}	2.70×10^{2}	93.88	-27.72
	0.18	6.72×10^{3}	1.03×10^{4}	91.07	-16.85
BSA	9.35	4.66×10^{5}	1.65×10^{5}	477.5	-32.36

Table S3 The major infrared absorption band of HA.

Wavenumber/cm^{-1}	Vibration
3429	-OH stretching
2926	asymmetric C-H stretching of aliphatic $–CH_2$,
	symmetric and asymmetric C-H stretching of $–CH_2$ and $–CH_3$
2851	symmetric C-H stretching of aliphatic $–CH_2$
1584	stretching of aromatic C=C,
	N-H deformation or C=N stretching of amides (amide II band)
1383	stretching of symmetric $-COO^-$,
	aliphatic -CH bending
1030	C-O stretching in polysaccharides

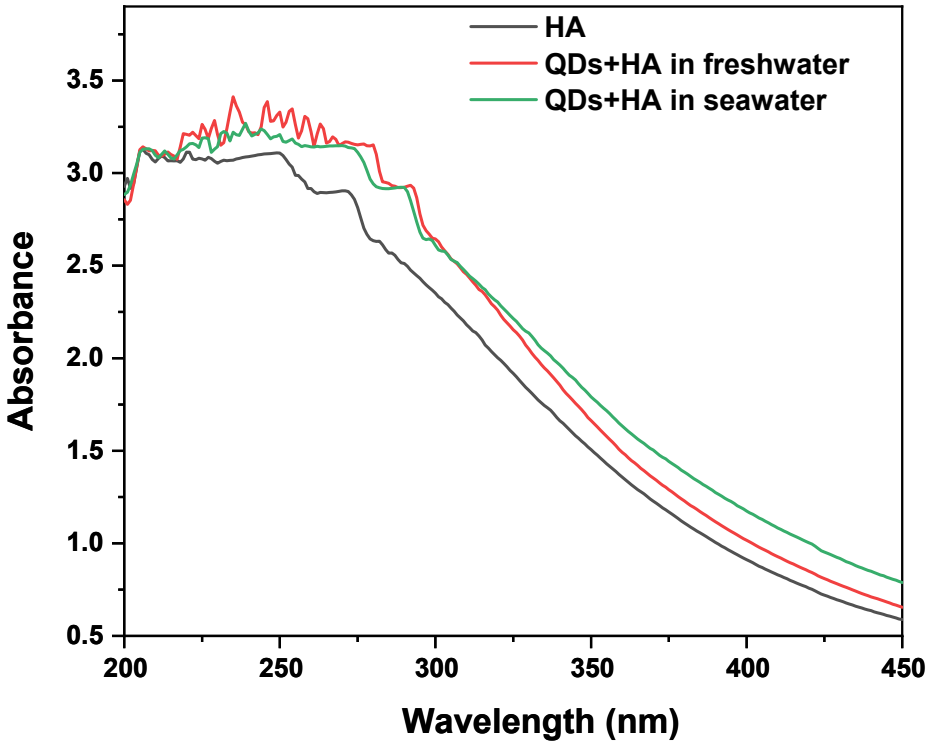

Fig. S6 UV-vis absorption spectra of HA and QDs-HA in seawater and freshwater. Conditions: c(HA)=100 mg/L, c(CdTe: Zn^{2+} QDs)=50 mg/L.

Table S4 The intensity of fluorescence peak of HA with and without CdTe: Zn^{2+} QDs.

System	Peak1		Peak2	
	Position $\lambda_{ex}/\lambda_{em}$ (nm/nm)	Intensity F	Position $\lambda_{ex}/\lambda_{em}$ (nm/nm)	Intensity F
HA in freshwater	400/400	1326	340/403	461
CdTe: Zn^{2+}QDs-HA in freshwater	400/400	4274	340/401	249.5
HA in seawater	400/400	1530	340/418	399.1
CdTe: Zn^{2+}QDs-HA in seawater	400/400	4149	350/415	240.6

References

Yu, W William, Lianhua Qu, Wenzhuo Guo, and Xiaogang Peng. 2003. Experimental determination of the extinction coefficient of CdTe, CdSe, and CdS nanocrystals, *Chemistry of materials*, 15: 2854-2860. https://doi.org/10.1021/cm034081k.

Yu, Yongli, Linru Xu, Jing Chen, Huanyu Gao, Shuo Wang, Jin Fang, and Shukun Xu. 2012. Hydrothermal synthesis of GSH–TGA co-capped CdTe quantum dots and their application in labeling colorectal cancer cells, *Colloids and Surfaces B: Biointerfaces*, 95: 247-253. https://doi.org/https://doi.org/10.1016/j.colsurfb.2012.03.011.